Highly Efficient Polymer White-Light-Emitting Diodes Based on Lithium Salts Doped Electron Transporting Layer

By *Fei Huang, Ping-I. Shih, Ching-Fong Shu, Yun Chi,* and *Alex K.-Y. Jen**

Organic white-light-emitting diodes (OWLEDs) have attracted considerable attention due to their potential applications in full-color flat panel displays, back-lighting sources for liquid-crystal displays, and solid-state lighting.[1–3] To achieve high-efficiency OWLEDs, efficient and balanced electron and hole injection and transport from cathode and anode are essential. This results in commonly used multilayer device structures, including the transparent conducting indium tin oxide (ITO) anode, hole-transport/injection layer (HTL), emissive layer (EML), electron-transport/injection layer (ETL), and metal cathode. For small molecule OWLEDs, this kind of multilayer structure can be easily produced by vacuum deposition with very thin emissive and transport layers to maximize light output and minimize power consumption of the devices. As a result, vacuum deposited OWLEDs have exhibited higher efficiencies than standard incandescent light sources (13–20 lm W^{-1}).[2–7] Polymer OWLEDs combining the advantages of simpler fabrication and lower production cost, especially for the large-area devices, are particularly attractive, because they can be fabricated by simple techniques like spin-coating or ink-jet printing.[8–20] However, it is very difficult to realize well-controlled multilayer device structures for polymer OWLEDs. Therefore, polymer OWLEDs often exhibit poorer performance than those obtained from small molecule OWLEDs. Only very few polymer OWLEDs reported so far have efficiencies comparable to that of the incandescent light bulbs.[14,19] Yang et al. have recently reported high-performance polymer OWLEDs with a power efficiency (PE) of 16 lm W^{-1} using Cs_2CO_3 as the electron-injection/hole blocking layer in the devices.[14] By using an alcohol-soluble conjugated polymer as ETL, we have also shown high-efficiency polymer phosphorescent OWLEDs with a PE of 14.5 lm W^{-1}.[19]

One of the most challenging problems for solution processed polymer OWLEDs is that their transport and emissive layers need to be thicker than those of the small molecule OWLEDs in order to minimize pinhole formation on the films and to balance the hole and electron recombination in the devices. Because most of the organic semiconductors possess relatively low carrier concentration and mobility,[21,22] thicker organic layers often result in increased driving voltage for the devices, and cause more power consumption. One way to overcome this limitation is to use doped HTL/ETL to enhance device performance.[23] Although p-doped poly(3,4-ethylene-dioxythiophene): poly(styrene sulfonic acid) (PEDOT:PSS) has been widely used in PLEDs to improve hole injection and transport, the successful development of n-doped materials for efficient electron injection and transport remains very challenging, due to the difficulty of finding suitable hosts and dopants.

Until recently, several water/alcohol soluble conjugated polymers were demonstrated to be good ETL materials for OLEDs. The polar groups on their side chains can form interfacial dipoles between the EML and metal cathode to enhance electron injection.[24–30] The unique solubility and excellent injection ability of these materials offer the possibility to improve electron injection and conduction by doping them with water-soluble alkali or alkaline earth-metal salts, which have been successfully used as n-dopants in OLEDs.[31–33] Among these materials, the newly developed water/alcohol-soluble neutral conjugated polymers are ideal hosts for n-doping, because they do not involve the complexity of the counter ions in conjugated polyelectrolytes.[19,30] In this Communication, we report highly efficient polymer OWLEDs derived from the Li_2CO_3-doped water/alcohol-soluble neutral conjugated polymer poly[9,9-bis(2-(2-(2-diethanolamino ethoxy)ethoxy)ethyl) fluorene] (PF-OH) ETL. It was found that the electron transporting ability of PF-OH ETL can be dramatically improved upon doping with Li_2CO_3 salt. Consequently, very-high-efficiency polymer OWLEDs with a maximum forward viewing luminous efficiency (LE) of 36.1 cd A^{-1} (61.4 cd A^{-1} for total viewing) and PE of 23.4 lm W^{-1} (39.8 lm W^{-1} for total viewing) were achieved, which is comparable to those reported from the state-of-the-art vacuum-deposited small-molecule OWLEDs.[2–7]

As shown in Scheme 1, the device configuration used in this study is ITO/PEDOT:PSS(30 nm)/FIrpic (7 wt%):Os-O (0.25 wt%):PVK:OXD-7(30 wt%) (70 nm)/ETL/Ba(4 nm)/Al (120 nm), where PEDOT:PSS is used as the hole-injecting/-transporting layer (HTL), sky-blue phosphorescent iridium complex bis[(4,6-di-fluorophenyl)-pyridinato-N,C^2] (picolinate) Ir(III) (FIrpic) and orange phosphorescent osmium complex (Os-O) are codoped into poly (*N*-vinylcarbazole) (PVK) host as the EML for white-light emission. 1,3-Bis[(4-*tert*-butylphenyl)-1,3,4-oxidiazolyl]phenylene (OXD-7) is incorporated to improve electron transport of the EML. Doped PF-OH (doped with

---

[*] Prof. A. K.-Y. Jen, Dr. F. Huang
Department of Materials Science and Engineering
Institute of Advanced Materials and Technology
University of Washington
Box 352120, Seattle, WA 98195-2120 (USA)
E-mail: ajen@u.washington.edu

Dr. P.-I. Shih, Prof. C.-F. Shu
Department of Applied Chemistry
National Chiao Tung University
Hsinchu, 300 (Taiwan ROC)

Prof. Y. Chi
Department of Chemistry, National Tsing Hua University
Hsin-Chu (Taiwan ROC)

DOI: 10.1002/adma.200802179

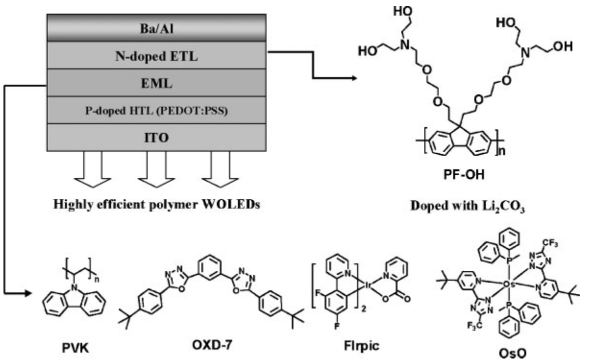

Scheme 1. Schematic of the device structure based on doped ETL and chemical structure of relevant materials.

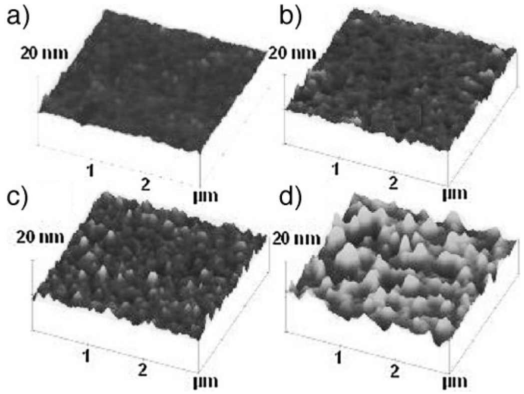

Figure 1. AFM images (3 μm × μm scale) of the PF-OH films spin-coated on top of the emissive layer. a) PF-OH, b) PF-OH doped with 5 wt% Li_2CO_3, c) PF-OH doped with 15 wt% Li_2CO_3, d) PF-OH doped with 30 wt% Li_2CO_3.

5 wt%, 15 wt%, 30 wt% Li_2CO_3) or undoped PF-OH are used as the ETL. The chemical structures of the relevant materials are shown in Scheme 1.

In our previous work, the optimal condition for processing neutral ETL materials in phosphorescent PLEDs was to use alcohol/water as cosolvent for spin-coating.[19,30] This facilitates the use of PF-OH as host for incorporating water-soluble alkali or alkaline earth-metal salts dopants, which have been successfully used as n-dopants in OLEDs.[31–33] Atomic force microscopy (AFM) was used to examine the quality of the doped PF-OH layer and possible crystallization from the doped salts, which may lead to phase separation and create rough surface features. As shown in Figure 1, the 5 wt% Li_2CO_3-doped PF-OH films exhibit a slightly rougher surface, with a root-mean-square surface roughness (rms) of 0.75 nm, compared to that of the undoped PF-OH films (rms = 0.53 nm), indicating Li_2CO_3 is well dispersed within the PF-OH film. However, when the concentration of the Li_2CO_3 is increased, the surface of the PF-OH films becomes rougher. The rms for 15 wt% and 30 wt% Li_2CO_3-doped PF-OH films increases to 1.3 and 2.7 nm, respectively, probably due to the formation of aggregates.

The typical current density–luminance–voltage (*J–L–V*) and luminous efficiency–power efficiency–current density (LE–PE–*J*) characteristics of the devices are shown in Figure 2. Clearly, the devices with Li_2CO_3-doped ETLs showed significantly higher current densities under the same driving voltage than that of the undoped device (Fig. 2a). The turn-on voltage (defined as the voltage where 1 cd m^{-2} is measured) of the OWLEDs decreased from 5.6 V for the device without doping to 5.3 V for device doped with 5 wt% Li_2CO_3, and further decreased to 4.8 V when the ETL was doped with 15 wt% Li_2CO_3 (Table 1). The increased current density and lowered turn-on voltage indicate that the transporting ability of PF-OH ETL is indeed enhanced upon doping with Li_2CO_3. As a result, the devices with doped ETLs exhibited much better performances than the ones without doping (Fig. 2 and Table 1). However, when the ETL was doped with 30 wt% Li_2CO_3, the device exhibited much poorer performance and *J–L–V* characteristics (Fig. 2 and Table 1). This indicates that the electrical properties of the PF-OH ETL are severely interfered under high doping concentrations, consistent with the morphological changes observed in the AFM study. The rougher surface showed the obvious formation of large aggregates (Fig. 1). Among all the devices, the device doped with 15 wt% Li_2CO_3 exhibited the best performance, with a maximum forward viewing LE of 36.1 cd A^{-1} and PE of 23.4 lm W^{-1} (Table 1). This corresponds to a maximum total viewing LE of 61.4 cd A^{-1} and PE of 39.8 lm W^{-1} for solid-state lighting applications, where all photons are taken into account for illumination.[5,18] Even at a practical surface luminance of 500 cd m^{-2}, the PE of the device was 23.3 lm W^{-1}, much higher than those obtained from the incandescent lighting sources. It should be pointed out that all devices exhibit stable white-light emission, and the corresponding Commission Internationale de l'Éclairage (CIE) coordinates are around (0.38,0.38) (Table 1), which is important for illumination applications. As shown in Figure 3, the CIE coordinates of the OWLED device (15 wt% Li_2CO_3 doped ETL) show a negligible shift from (0.38,0.38) at 8 V (4.97 mA cm^{-2}, 1400 cd m^{-2}) to (0.36,0.38) at 14 V (190 mA cm^{-2}, 17000 cd m^{-2}). To the best of our knowledge, the performance of these devices are among the highest reported to date for polymer-based phosphorescent OWLEDs,[8–20] and are comparable with those reported for small-molecule OWLEDs.[2–7]

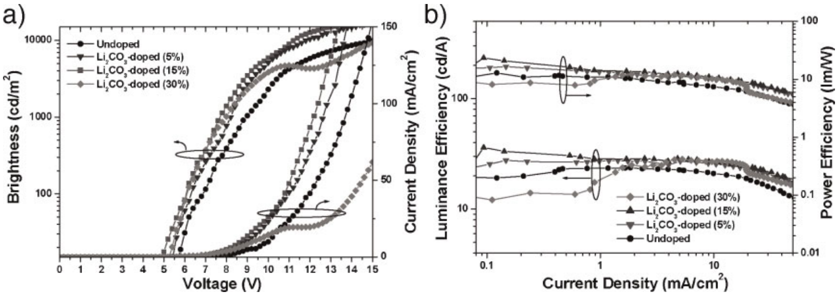

Figure 2. a) *J–L–V* characteristics and b) LE and PE versus current density characteristics of the devices with different ETLs.

Table 1. Device performance (forward-viewing) of OWLEDs using different ETL in the device configuration: ITO/PEDOT:PSS/FIrpic(7 wt%):Os-O(0.25 wt%):PVK:OXD-7(30 wt%)/ETL/Ba/Al.

Device with different ETL	Non-doped PF-OH	Li_2CO_3-doped PF-OH	Li_2CO_3-doped PF-OH	Li_2CO_3-doped PF-OH
Dopant concentration	0 wt %	5 wt %	15 wt %	30 wt %
Turn-on voltage (V)	5.6	5.3	4.8	5.2
E.Q.E. (%)[a]	9.2	10.5	12.6	6.9
L.E. (cd A^{-1})[a]	22.7	26.7	32.0	18.1
P.E. (lm W^{-1})[a]	11.7	15.1	18.5	9.5
Max brightness (cd m^{-2})	10720 (@ 16 V)	18200 (@ 17 V)	19580 (@ 16 V)	10800 (@ 16 V)
Max E.Q.E. (%)	9.4	10.8	14.2	11.1
Max L.E. (cd A^{-1})	23.7	27.6	36.1	27.7
Max P.E. (lm W^{-1})	12.9	16.6	23.4	12.2
V_{oc}	2.0	2.0	2.0	1.9
CIE, x and y[b]	0.39 and 0.39	0.38 and 0.38	0.38 and 0.38	0.37 and 0.38

[a] Recorded at 100 cd m^{-2}. [b] At 8 V.

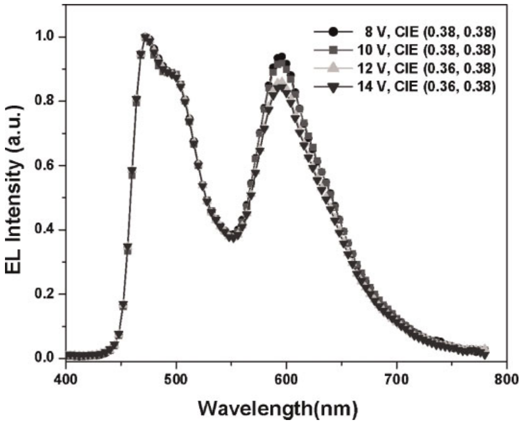

Figure 3. Normalized EL spectra of OWLED with 15 wt% Li_2CO_3 doped ETL at various driving voltages.

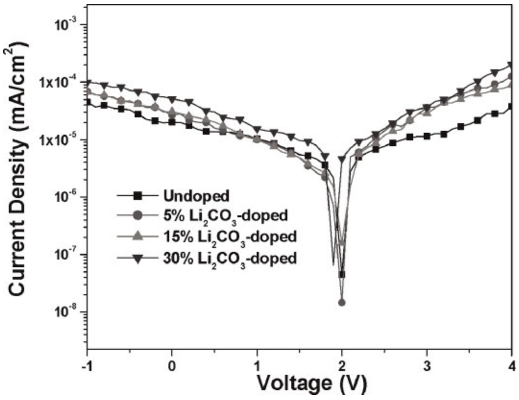

Figure 4. Photovoltaic characteristics of devices with different ETLs.

The significantly improved device performance originates from the improved current density of PF-OH ETL upon doping. There are two possible mechanisms that may contribute to this effect: either the improved charge transport[23] or the improved electron-injection ability of the PF-OH ETL from the metal cathode upon doping.[34] To clarify this, photovoltaic (PV) measurements were performed to obtain open circuit voltage (V_{oc}) across the devices, which is primarily influenced by the effective work function of the cathode and can reflect the electron-injection ability of the ETL materials.[26,28] As shown in Figure 4, all the devices exhibit a similar V_{oc}, at around 2.0 V, which indicates that the electron-injection ability of PF-OH ETL is not improved upon doping. Therefore, the greatly improved performance of doped devices should be mainly due to the enhanced charge-transporting ability of PF-OH ETL upon doping. To verify this, two kinds of single-carrier devices based on the electron-dominated device (ITO/Al (100 nm)/PVK:OXD-7 (30 wt%) (70 nm)/ETL (20 nm)/Ba (4 nm)/Al (100 nm)) and the hole-dominated device (ITO/PEDOT (30 nm)/PVK:OXD-7 (30 wt%) (70 nm)/ETL (20 nm)/Au (100 nm)), were fabricated. As shown in Figure 5a, in the electron-dominated devices the electron current density of the devices with Li_2CO_3-doped ETLs are much higher than those of

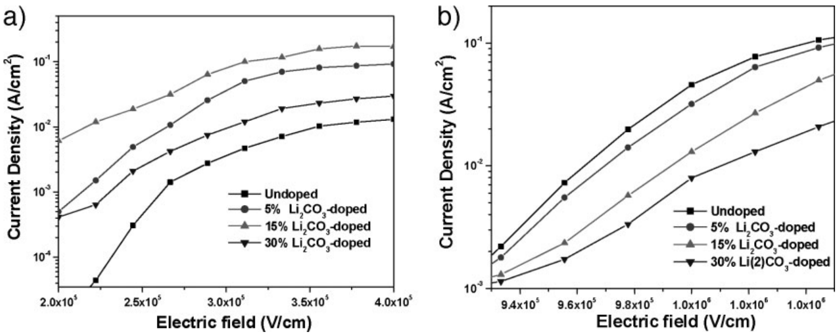

Figure 5. Current density versus electric field intensity characteristics of the single-carrier devices: a) electron-dominated device, b) hole-dominated device.

the devices with undoped ETL. This means the electron-transporting ability of PF-OH is indeed significantly enhanced upon doping. The device with 15 wt% Li_2CO_3-doped ETL has the highest current density under the same electric-field intensity compared to others, indicating 15 wt % doping is the optimal condition to improve the electron-transporting ability. This is consistent with previously mentioned device results (Fig. 2 and Table 1). More interestingly, the results of the hole-dominate device clearly showed that the current density of the hole carriers in PF-OH ETLs significantly decreased upon doping. Thereby, all these results clearly indicate that a Li_2CO_3-doped PF-OH ETL possesses an enhanced electron-transport/hole-blocking ability compared to that of the undoped PF-OH ETL, resulting in much improved device performance.

In conclusion, we report efficient polymer OWLEDs based on a water/alcohol-soluble neutral ETL doped with Li_2CO_3 salt. The results from the single-carrier devices indicate that the electron-transport/hole-blocking properties of PF-OH ETLs can be dramatically improved upon doping. The resulting solution-processed polymer OWLED showed a maximum forward viewing LE of 36.1 cd A^{-1} (61.4 cd A^{-1} for total viewing) and a PE of 23.4 lm W^{-1} (39.8 lm W^{-1} for total viewing), which is comparable to those reported from the state-of-the-art vacuum-deposited small-molecule OWLEDs.

Experimental

Polymer OWLED devices were fabricated in the following configuration: ITO/PEDOT:PSS/emissive layer/ETL (PF-OH-based)/Ba/Al. All devices were fabricated on ITO with a sheet resistance of 10–20 Ω/sq. The ITO-coated glass substrates were ultrasonically cleaned with detergent, deionized water, acetone, and isopropyl alcohol. A layer of 40 nm thick PEDOT:PSS (H. C. Stack, 4083) was spin-coated onto the precleaned and O_2-plasma-treated ITO substrates. The PEDOT:PSS layer was first baked at 100 °C for 0.5 h to remove residual water, and then moved into a glovebox under the argon-protected environment to perform the subsequent multilayer integration process. The PVK host and Li_2CO_3 were purchased from Aldrich. FIrpic and OXD-7 were purchased from the American Dye Sources Inc. FIrpic, OXD-7, and PVK were dissolved in chlorobenzene, respectively. Os-O was prepared according to a previously reported procedure [35]. A mixture of 7 wt% Firpic, 0.25 wt% Os-O, and 30 wt% OXD-7 was doped into a PVK host and spin-cast onto PEDOT as the emissive layer. The samples were annealed at 120 °C for 0.5 h to remove residual solvent. The thickness of the emissive layer was 70 nm. The ETL was composed of PF-OH and Li_2CO_3. PF-OH was dissolved in a mixed solvent of water/methanol (1/4 v/v). 5–30 wt% Li_2CO_3 was added to the prepared PF-OH solution, which was spin-coated onto the emissive layer to yield films with 20 nm thickness, followed by drying inside the glovebox at 100 °C for 10 min. Finally, a 4 nm thick film of Ba and a 120 nm thick film of Al were thermally evaporated on top of the ETL as a cathode under vacuum (1.3×10^{-4} Pa). The device testing was carried out in air at room temperature. EL spectra were recorded using a Oriel Instaspec IV spectrometer with a charge-coupled device (CCD) detector. Current–voltage (I–V) characteristics were measured using a Hewlett-Packard 4155B semiconductor parameter analyzer. The power of the EL emission in the normal direction of the ITO side was measured using a calibrated Si-photodiode and a Newport 2835-C multifunctional optical meter. Photometric units (cd m^{-2}) were calculated using the forward output power together with the EL spectra of the devices under assumption of the emission's Lambertian space distribution. For the measurements of photocurrent versus voltage characteristics, the PLEDs were exposed to light with intensity of 100 mW cm^{-2} from a simulated AM1.5 light source (Oriel Co.). Open-circuit voltages of those PLEDs were thus derived from the zero current point on the photocurrent–voltage curves.

Acknowledgements

F. Huang and P.-I. Shih contributed equally to this work. Financial supports from the National Science Foundation (NSF-STC Program under Agreement Number DMR-0120967) and the Boeing-Johnson Foundation are acknowledged.

Received: July 28, 2008
Revised: September 26, 2008

---

[1] J. Kido, M. Kimura, K. Nagai, *Science* **1995**, *267*, 1332.

[2] B. W. D'Andrade, S. R. Forrest, *Adv. Mater.* **2004**, *16*, 1585.

[3] A. Misra, P. Kumar, M. N. Kamalasanan, S. Chandra, *Semicond. Sci. Technol.* **2006**, *21*, R35.

[4] B. W. D'Andrade, R. J. Holmes, S. R. Forrest, *Adv. Mater.* **2004**, *16*, 624.

[5] Y. R. Sun, N. C. Giebink, H. Kanno, B. W. Ma, M. E. Thompson, S. R. Forrest, *Nature* **2006**, *440*, 908.

[6] H. Kanno, R. J. Holmes, Y. Sun, S. Kena-Cohen, S. R. Forrest, *Adv. Mater.* **2006**, *18*, 339.

[7] E. L. Williams, K. Haavisto, J. Li, G. E. Jabbour, *Adv. Mater.* **2007**, *19*, 197.

[8] J. Kido, H. Shionoya, K. Nagai, *Appl. Phys. Lett.* **1995**, *67*, 2281.

[9] X. Gong, W. Ma, J. C. Ostrowski, G. C. Bazan, D. Moses, A. J. Heeger, *Adv. Mater.* **2004**, *16*, 615.

[10] X. Gong, S. Wang, D. Moses, G. C. Bazan, A. J. Heeger, *Adv. Mater.* **2005**, *17*, 2053.

[11] J. X. Jiang, Y. H. Xu, W. Yang, R. Guang, Z. Q. Liu, H. Y. Zhen, Y. Cao, *Adv. Mater.* **2006**, *18*, 1769.

[12] T. H. Kim, H. K. Lee, O. O. Park, B. D. Chin, S. H. Lee, J. K. Kim, *Adv. Funct. Mater.* **2006**, *16*, 611.

[13] P. I. Shih, Y. H. Tseng, F. I. Wu, A. K. Dixit, C. F. Shu, *Adv. Funct. Mater.* **2006**, *16*, 1582.

[14] J. Huang, G. Li, E. Wu, Q. Xu, Y. Yang, *Adv. Mater.* **2006**, *18*, 114.

[15] Y. H. Niu, M. S. Liu, J. W. Ka, J. Bardeker, M. T. Zin, R. Schofield, Y. Chi, A. K.-Y. Jen, *Adv. Mater.* **2007**, *19*, 300.

[16] J. Liu, Z. Y. Xie, Y. X. Cheng, Y. H. Geng, L. X. Wang, X. B. Jing, F. S. Wang, *Adv. Mater.* **2007**, *19*, 531.

[17] F. I. Wu, X. H. Yang, D. Nether, R. Dodda, Y.-H. Tseng, C. F. Shu, *Adv. Funct. Mater.* **2007**, *17*, 1058.

[18] H. B. Wu, J. H. Zou, F. Liu, L. Wang, A. Mikhailovsky, G. C. Bazan, W. Yang, Y. Cao, *Adv. Mater.* **2008**, *20*, 696.

[19] Y. Zhang, F. Huang, Y. Chi, A. K.-Y. Jen, *Adv. Mater.* **2008**, *20*, 1565.

[20] Y. Zhang, F. Huang, A. K.-Y. Jen, Y. Chi, *Appl. Phys. Lett.* **2008**, *92*, 063303.

[21] Y. Shirota, H. Kageyama, *Chem. Rev.* **2007**, *107*, 953.

[22] V. Coropceanu, J. Comil, D. A. S. Filho, Y. Olivier, Y. Silve, J.-L. Brédas, *Chem. Rev.* **2007**, *107*, 926.

[23] K. Walzer, B. Maennig, M. Pfeiffer, K. Leo, *Chem. Rev.* **2007**, *107*, 1233.

[24] F. Huang, L. T. Hou, H. B. Wu, X. H. Wang, H. L. Shen, W. Cao, W. Yang, Y. Cao, *J. Am. Chem. Soc.* **2004**, *126*, 9845.

[25] F. Huang, H. B. Wu, D. L. Wang, W. Yang, Y. Cao, *Chem. Mater.* **2004**, *16*, 708.

[26] H. B. Wu, F. Huang, Y. Q. Mo, W. Yang, D. L. Wang, J. B. Peng, Y. Cao, *Adv. Mater.* **2004**, *16*, 1826.

[27] W. L. Ma, P. K. Iyer, X. Gong, B. Liu, D. Mose, G. C. Bazan, A. J. Heeger, *Adv. Mater.* **2005**, *17*, 274.

[28] R. Q. Yang, H. B. Wu, Y. Cao, G. C. Bazan, *J. Am. Chem. Soc.* **2006**, *128*, 14422.

[29] S. H. Oh, S. I. Na, Y. C. Nah, D. Vak, S. S. Kim, S. D. Y. Kim, *Org. Electron.* **2007**, *8*, 773.

[30] F. Huang, Y. H. Niu, Y. Zhang, J. W. Ka, M. S. Liu, A. K.-Y. Jen, *Adv. Mater.* **2007**, *19*, 2010.

[31] T.-W. Lee, T. Noh, B.-K. Choi, M.-S. Kim, D. W. Shin, J. Kido, *Appl. Phys. Lett.* **2008**, *92*, 043301.

[32] K. R. Choudhury, J.-h. Yoon, F. So, *Adv. Mater.* **2008**, *20*, 1456.

[33] C. C. Hsiao, A. E. Hsiao, S. A. Chen, *Adv. Mater.* **2008**, *20*, 1982.

[34] L. S. Hung, C. W. Tang, M. G. Mason, *Appl. Phys. Lett.* **1997**, *70*, 152.

[35] Y.-L. Tung, *Ph. D. Thesis*, National Tsing Hua University, Hsinchu, Taiwan **2005**.